0031-3998/07/6203-0248
PEDIATRIC RESEARCH

Vol. 62, No. 3, 2007
Printed in U.S.A.

ARTICLES

Temporal and Regional Evolution of Aquaporin-4 Expression and Magnetic Resonance Imaging in a Rat Pup Model of Neonatal Stroke

JÉRÔME BADAUT, STEPHEN ASHWAL, BEATRIZ TONE, LUCA REGLI, HOU ROU TIAN, AND ANDRE OBENAUS

Neurosurgery Research Group [J.B., L.R.], Centre Hospitalier Universitaire Vaudois (CHUV), 1011 Lausanne, Switzerland; Department of Pediatrics [S.A., B.T., H.R.T.], Department of Radiation Medicine [A.O.], Loma Linda University, School of Medicine, Loma Linda, California 92354

ABSTRACT: Edema formation can be observed using magnetic resonance imaging (MRI) in patients with stroke. Recent studies have shown that aquaporin-4 (AQP4), a water channel, is induced early after stroke and potentially participates in the development of brain edema. We studied whether induction of AQP4 correlated with edema formation in a rat pup filament stroke model using high field (11.7-Tesla) MRI followed by immunohistochemical investigation of AQP4 protein expression. At 24 h, we observed increased T2 values and decreased apparent diffusion coefficients (ADC) within injured cortical and striatal regions that reflected the edema formation. Coincident with these MR changes were significant increases in AQP4 expression on astrocytic end-feet in the border regions of injured tissues. Striatal imaging findings were still present at 72 h with a slow normalization of AQP4 expression in the border regions. At 28 d, AQP4 expression normalized in the border while in this region ADC values increased. We show that induction of AQP4 is increased during the period of active edema formation in the border region without regional correlation with edema. Finally, induction of AQP4 on astrocyte end-feet could participate in tissue preservation after ischemia in the immature rat brain. **(*Pediatr Res* 62: 248–254, 2007)**

Arterial ischemic stroke, often within the distribution of the MCA, occurs in approximately 1 per 4,000 neonates and as in adults there are significant sequelae over the lifespan that make this disease an important public health concern (1). Increasingly, magnetic resonance imaging (MRI) is used to evaluate neonatal ischemic brain injury and several recent studies have demonstrated the added value of DWI in assessing injury severity and in determining long-term outcome (2–4). MRI also has been used to visualize brain edema that contributes to the morbidity and mortality of many of these conditions (5). In general, diffusion restriction with reduced ADC values correlates with cytotoxic edema, whereas increased T2WI values reflects the development of vasogenic edema (6,7).

In the past decade, attention has focused on AQP in the development of brain edema. AQP are water-specific channels that provide a direct water route through the plasma membrane and are important in the regulation of water movement. Expression of AQP4 and AQP9, detected in mammalian brain, is altered in several conditions, including ischemia (7–9). Although astrocytic expression of AQP4 and AQP9 increases after ischemia, only AQP4 expression temporally correlates with the evolution of brain edema in adult mice and suggests that regulation of AQP4 expression could be a potential therapeutic target (9).

The role of AQP4 in the evolution of cytotoxic and vasogenic edema after stroke remains uncertain. In the adult mouse, increased astrocytic AQP4 expression was observed at 1 h and 48 h after stroke (9). In contrast to adult stroke model studies, investigations in a neonatal rat pup model of HII found that AQP4 expression (decreased at 1 h and 24 h after HII), was associated with decreased ADC (*i.e.* presumed cytotoxic edema) and increased T2WI values (*i.e.* presumed vasogenic edema) (7). Functional studies in adult knockout mice have shown that deletion of AQP4 diminishes cytotoxic edema formation and improves neurologic outcome (10). However, AQP4 appears also to be essential in reducing the duration and onset of vasogenic edema by facilitating water clearance (11,12). Thus, there are conflicting findings regarding the expression and role of AQP4 that relate to development (adult *versus* pup) as well as the model used (stroke *versus* HII). Increased astrocytic AQP4 expression in the border regions after stroke (9) also has raised the question

Received September 27, 2006; accepted April 5, 2007.

Correspondence: Jérôme Badaut, Ph.D., Neurosurgery Research Group, Centre Hospitalier Universitaire Vaudois, Pavillon 3 – Beaumont, 1011 Lausanne, Switzerland; e-mail: Jerome.Badaut@chuv(CHUV).ch

Supported in part by the Pediatric Research Fund, Department of Pediatrics, and a NASA Cooperative Agreement NCC9-149 to the Radiobiology Program, Department of Radiation Medicine at Loma Linda University, the Swiss Science Foundation (FN 3100AO-108001); SwissHeart Foundation; Fondazione Per Lo Studio Delle Malattie Neurodegenerative Delle Persone Adulte e Dell' Anziano, from Lugano, Switzerland.

Abbreviations: ADC, apparent diffusion coefficients; **AQP,** aquaporins; **AQP4-IR,** AQP4-immunoreactivity; **DWI,** diffusion-weighted imaging; **HII,** hypoxic-ischemic injury; **MCA,** middle cerebral artery; **T2WI,** T2-weighted imaging; **tfMCAO,** transient filament middle cerebral artery occlusion

Table 1. *Percentage survival and MRI-based hemispheric ischemic injury*

	24 h	72 h	28 d
Survival (%)	64	64	23
Total hemisphere infarcted (%)			
DWI	46.3 ± 4.9	22.3 ± 4.7	10.4 ± 5.0
T2	—	38.9 ± 6.5	10.3 ± 3.3

whether this increase contributes to or ameliorates postischemic edema.

To gain insight into the role of AQP4 in the development and evolution of cerebral edema in neonatal stroke, we have serially (*i.e.* at 24 h, 72 h, and 28 d) studied the regional profile of AQP4 expression relative to MRI findings after transient focal ischemia in the rat pup. The presence of increased AQP4 labeling in brain regions with less edema, as visualized by MRI, suggests that AQP4 induction in astrocyte end-feet limits edema formation by facilitating water clearance from/to the vascular compartment.

METHODS

Transient filament MCA occlusion. Focal ischemia in the rat pup was accomplished using a filament model of temporary unilateral proximal occlusion of the left middle cerebral artery (MCA, Table 1) (13). Unsexed 10-d-old spontaneously hypertensive rat pups (14–18 g; $n = 13$) were anesthetized with 4% isoflurane in a mixture of 40% oxygen:60% air, and body temperature was maintained at 37°C during surgical procedures and recovery until locomotor activity returned. Through a midline neck incision, three vessels were cauterized, a small incision in the external carotid artery allowed a nylon filament (#6.0, 0.07 mm, silicone-coated tip) to be advanced into the internal carotid to block the MCA. At the end of the 90-min occlusion period, the pup was checked for neurologic deficits, reanesthetized, the filament was removed, and the surgical site closed. The pup was then transferred to the MRI scanner.

MRI and analysis. Two imaging data sets were acquired on a Bruker 11.7 T MRI (Bruker Biospin, Billerica, MA): 1) a 10 echo T2, and 2) a diffusion-weighted sequence (14). The T2 sequence had the following parameters: a TR/TE of 4600 ms/10.2 ms, a 128 × 128 matrix, a 3-cm field of view (FOV), and two averages (NEX) for a total acquisition time of 20 min. The spin echo diffusion sequence had a TR/TE of 3000 ms/25 ms, two b-values (0.72, 1855.64 s/mm^2), 128 × 128 matrix, 3 cm FOV, and two averages for 17 min. Due to the size increase of the rat pup at 28 d, imaging was conducted on our larger bore Bruker 4.7T imager, using identical imaging parameters. An RF (radiofrequency) volume coil was used for all imaging.

All MR data sets were quantified using standard previously published protocols (13). Briefly T2 relaxation rates were determined by varying the echo time (TE) from 10 to 100 ms. Coefficients were determined from exponential fits for each pixel of the T2 data series to generate T2 maps. ADC maps were calculated using a linear two-point fit (14).

ROI analysis for T2WI and DWI included both ipsi- and contralateral to the lesion primary regions of the rodent brain: cortex, striatum, and border areas. ROI analysis was performed on a single slice at the same level as the histology (Fig. 1) with a box placed in the ROI (13). Cheshire image processing software (Hayden Image /Processing Group, Waltham, MA) was used to outline the anatomical ROI, which were then overlaid onto corresponding T2 and ADC maps. The mean, SD, number of pixels, and region for each animal was extracted and summarized in a spreadsheet.

Histology and immunohistochemistry. Based on a previous serial MRI study, 24 h ($n = 4$) and 72 h ($n = 6$) (maximal ischemic changes) and 28 d ($n = 3$) after stroke were selected (13). Animals were deeply anesthetized with ketamine 90 mg/kg and xylazine 10 mg/kg by intraperitoneal injection and perfused transcardially with 10% buffered neutral formalin solution. Brains were removed, post fixed in the same fixative overnight. Tissue was embedded in paraffin with 7-μm thick sections from each block cut on a microtome and mounted onto glass slides. Every 10th section was mounted on gel-chrome-alum coated slides and stained with 0.1% cresyl violet acetate (Fig. 1) (13).

AQP4 immunolabeling was evaluated on serial slices corresponding to the MRI acquisitions (9). After epitope retrieval, immunostaining was carried out in PBS containing 0.1% Triton X-100 and 1% BSA. After each incubation, sections were rinsed in PBS 3 × 10 min. For single immunolabeling, the sections were incubated overnight at 4°C with anti-AQP4 (1/200, Chemicon International, Temecula, CA) and then with an infrared-Dye-800-nm secondary anti-rabbit (1/1000, Roche Molecular Biochemicals, Indianapolis, IN) for 2 h at room temperature. Sections were scanned with an infrared scanner and fluorescence was quantified (Odyssey-system, LiCor, Germany). The linear relationship between the concentration of the AQP4 and fluorescence signal was established on control sections incubated with different dilutions of anti-AQP4
($r^2 = 0.94$) (14). The fluorescence from AQP4-immunoreactivity (AQP4-IR) was quantified with three boxes placed in ipsilateral and contralateral cortices and striatum and the border region (frontal cortex and septum) in two slices per rats (Fig. 1*A*). The border region was defined as the area adjacent to the brain region where both the ADC and T2 values were altered. Fluorescence was converted in integrated-intensities and expressed in percent of the contralateral regions.

For the double immunohistochemistry, sections were incubated with a mixture of anti-AQP4 and anti-GFAP (Sigma Chemical Co., 1/400) overnight at 4°C and then with a mixture of anti-rabbit coupled to CY3 (1/300, Jackson Immunoresearch, West Grove, PA) and anti-mouse coupled to FITC (1/200, Jackson Immunoresearch) for 2 h at room temperature (9). The epifluorescence of FITC and CY3 were successively recorded through separate channels using Fluo-up (Explora-Nova, La Rochelle, France) set-up on epifluorescence microscope (Olympus).

Statistical analysis. Comparisons between contra- and ipsilateral T2 and DWI was statistically evaluated at each time point using a *t* test (SigmaStat, SPSS Inc., Chicago, IL; $p < 0.05$) and data are presented as as the mean ± SEM. Immunohistochemical data are presented as the mean ± SEM and the statistical analysis was done using GraphPad InStat (GraphPad Software, San

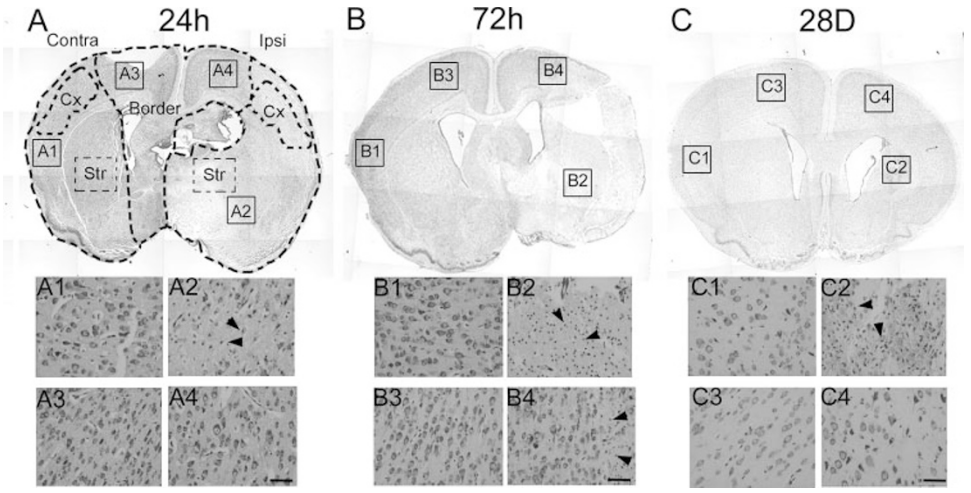

Figure 1. Serial histologic sections from animals at 24 h (*A*), 72 h (*B*), and 28 d (*C*) after stroke onset. (*A–C*) Low-magnification cresyl violet stained sections showing a decrease in cell density in ischemic (ipsi, *A2*) compared with border regions (*A3, A4*) and the contralateral hemisphere (*A1*). At higher magnification, normal cell density was observed in contralateral compared with ischemic regions (*A1–C1*), where pyknotic cells were observed. In the border region at 72 h (*B*), normal neuronal cell bodies were observed (*A3, C3*) except at 72 h where occasional pyknotic cells (*arrowheads*) were adjacent to the ischemic region (*B4*). Bar = 40 μm, Cx, cortex; St, striatum.

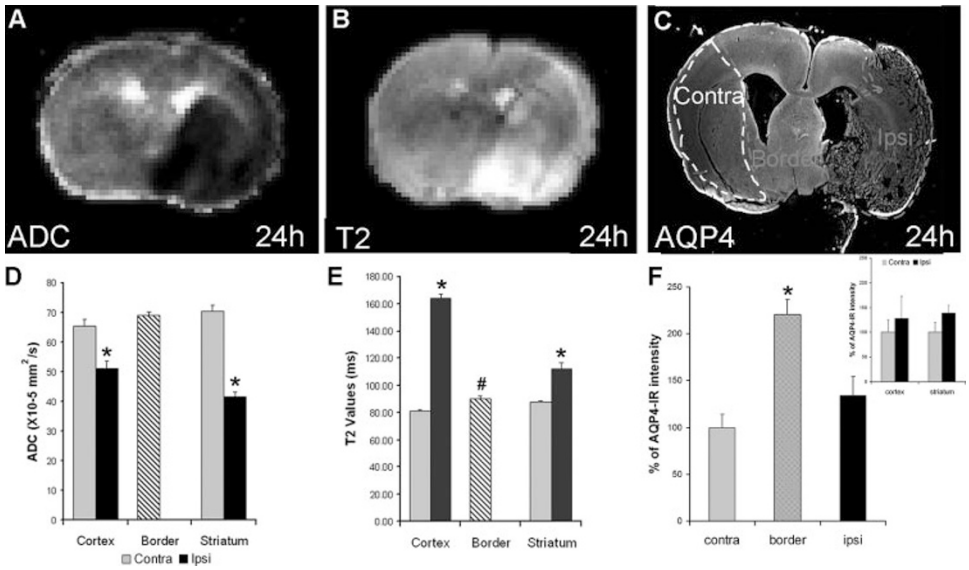

Figure 2. Macroscopic comparison of MRI data and AQP4 immunohistochemistry at 24 h after tfMCAO occlusion. (*A*) Representative ADC-image showing decreased diffusion within the ischemic region. (*B*) A T2WI from the same animal shows increased signal intensities in the injury, suggestive of edema formation. (*C*) AQP4 staining intensity in the same rodent showed increased AQP4 expression in the border region. (*D*) ADC showed decreased diffusion in the ipsilateral cortex and striatum, consistent with neuronal and glial swelling. (*E*) Concomitant increases in T2-values (increased water content) occurred at the same time in the ipsilateral ischemic tissue. (*F*) Quantification of AQP4 in the cortex and striatum (*inset*) showed elevated AQP4-IR levels. AQP-IR in the border region was significantly increased when compared with the contralateral (*contra,* $p < 0.001$) and ipsilateral (*ipsi,* $p < 0.01$) tissues.

Diego, CA). AQP-IR data were compared by a paired *t* test and Tukey-Kramer Multiple Comparisons Test.

RESULTS

24 hours. There were significant changes in ADC and T2WI at 24h after tfMCAO (Fig. 2, *A* and *B*) in cortical and striatal regions in the affected hemisphere. ADC showed decreased signal intensity within the affected cortex and striatum. ADC values, a measure of water mobility (that suggests cytotoxic edema when reduced), were decreased in cortex (22%) and striatum (41%) but not in the border region (defined in Fig. 1; Fig. 2, *A* and *D*). T2WI signal intensity and values (that suggests vasogenic edema when elevated) in cortical regions were significantly increased respectively by 101% and 81% in the ipsilateral compared with the contralateral cortex and border region (Fig. 2, *B* and *E*; $p < 0.001$). A smaller increase in T2WI values (28%, $p < 0.001$) was also observed in the striatum. It is important to note that the ADC shows a larger region of signal change compared with the T2WI at 24 h. This reflects the evolution of the ischemic injury, where cell death, edema formation, and gliosis are occurring at different rates and magnitudes in different brain regions. The MRI data suggest that ongoing cellular swelling and edema formation are present at 24 h.

Regional AQP4-IR was significantly altered at 24 h (Fig. 2*C*, $n = 3$). The AQP4-IR intensities were higher in injured cortex and striatum than in corresponding contralateral regions (Fig. 2*F*). Within the border region the ADC values are similar to the contralateral cortex/striatum ($p = 0.16$) and T2WI is increased by 6% in the border region ($p < 0.01$) compared with the contralateral cortex. In this border region, AQP4-IR intensity was greater (220 ± 16%) compared with the contralateral region (100 ± 14%, $p < 0.001$) and to the ipsilateral cortical and striatal regions (134 ± 21%, $p < 0.01$) (Fig. 2*F*). Therefore, maximal AQP4 induction was observed in brain regions where there was no evidence of cytotoxic (*i.e.* decreased ADC) or vasogenic (increased T2WI) edema.

At the cellular level (Fig. 3), AQP4-IR induction was observed around blood vessels and on GFAP-positive astrocyte processes (Fig. 3, *A1* and *A2*) in the lesion. In the border region, AQP4 induction was only observed on astrocyte endfeet around blood vessels (Fig. 3, *B* and *C*). The greatest intensity for AQP4-IR was observed in brain regions in the vicinity of the ipsilateral cortex (Fig. 3*B*) and striatum (not shown). In the contralateral cortex (Fig. 3, *C* and *D*), AQP4 staining around blood vessels was lower than in the ipsilateral cortex but staining was higher in the contralateral frontal cortex (Fig. 3*C*) than in the contralateral parietal cortex (Fig. 3*D*). This latter region was considered a control region. These findings suggest that there is a gradual change for AQP4 induction from the ipsilateral region of ischemic injury to the contralateral hemisphere (Fig. 3, *B–D*).

72 hours. At 72 h, ADC values normalized within cortical regions but decreased within the striatum (15%, $p < 0.008$, Fig. 4, *A* and *D*). At 72 h, T2WI signal intensities were considerably elevated compared with 24 h (Fig. 2*B*). The T2 values in cortical regions were 33% ($p < 0.001$) and striatal regions were 103% greater compared with the contralateral hemisphere ($p < 0.001$, Fig. 4*E*). This is in marked contrast to the changes at 24 h, in which cortical regions (101%) showed a much greater increase than the striatum (28%). This reciprocal change in T2WI values was not reflected in the ADC data. At this time point, neuropathological changes (cellular swelling, onset of cell death) are thought to be nearing completion while edema formation is now well advanced, as reflected by the increased T2WI values. These findings sug-

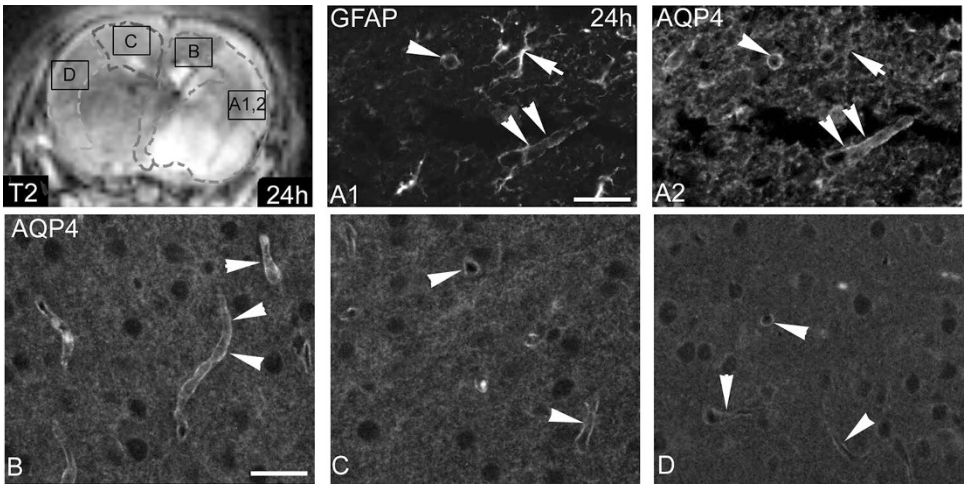

Figure 3. (*A*) T2-images, at 24 h after stroke onset, were used to localize the regions of interest. In ipsilateral cortex GFAP-IR (*A1*) was co-localized with AQP4-staining (*A2*) around blood vessels (*arrowheads*) and on processes (*arrows*). (*B*) The intensity of the AQP4 staining was significantly increased around blood vessels (*arrowheads*) in the cortical tissues where ADC was decreased and T2-values were increased. (*C*) In the frontal cortex of the contralateral hemisphere the intensity of AQP4-IR around blood vessels (*arrowheads*) was higher than in the contralateral parietal cortex (*arrowheads, D*). Bar: *A–D* = 40 μm.

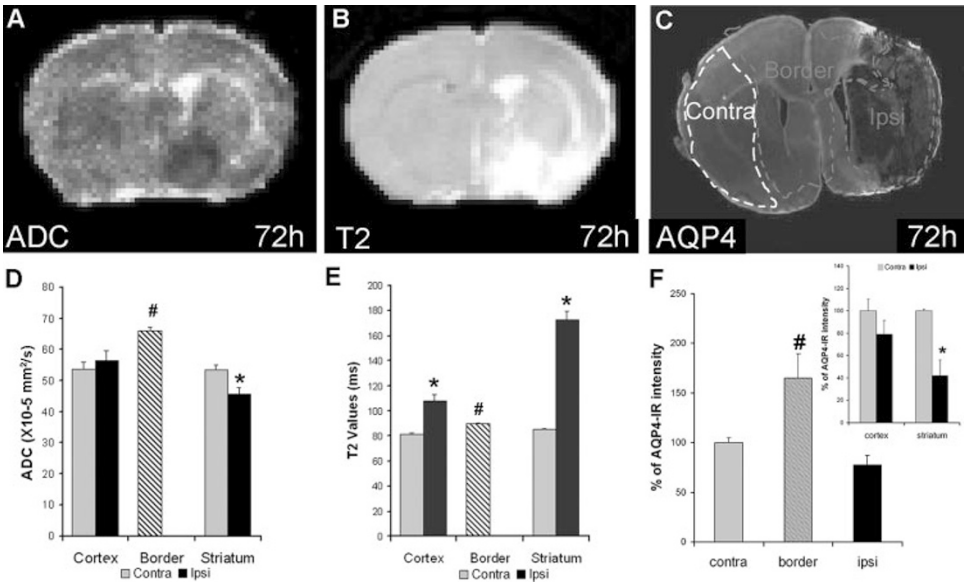

Figure 4. Comparison of MR data with AQP4 labeling at 72 h after ischemia. (*A*) ADC-image illustrates partial resolution of the high-intensity changes observed at 24 h. (*B*) At this time point, the T2 values continue to increase and suggest increased vasogenic edema. (*C*) Illustration of the AQP4-IR intensity with decreased lesional staining. (*D*). ADC quantification showed normalization of diffusion in the cortex with moderate decreases remaining in the striatum. (*E*) In contrast to 24 h, the T2 values are decreased in cortical regions but the striatum had a large increase in water content. (*F*) The level of expression of AQP4 was significantly decreased in the ipsilateral cortex and striatum (*F, inset,* $*p < 0.01$). More detailed analysis showed that in the border regions the level of AQP4 was still significantly increased ($\#p < 0.05$) and was different from values measured in the ipsilateral cortex and striatum.

gest early vasogenic edema in the cortex that decreases by 72 h, whereas at 72 h there is an increase in striatal vasogenic edema. In addition, volumetric analysis from DWI and T2-images showed a hemispheric lesion volume of 22.3 ± 4.7% (Table 1).

AQP4-IR was decreased in the ipsilateral compared with the contralateral striatum (42 ± 14%, $p < 0.05$) (Fig. 4, *C* and *F, inset*, $n = 4$) as well as in cortical regions (79 ± 12%). The relative decrease in cortical AQP4 expression at 72 h is vastly different from the increase in AQP4-IR at 24 h (128 ± 44%, Fig. 2, *F, inset*). At 72 h, ADC and T2WI values were increased by 23% ($p < 0.001$) and 8% ($p < 0.001$), respectively, in the border region compared with contralateral cortex and striatum. AQP4-IR was also elevated compared with contralateral and ipsilateral regions (Fig. 4*C*). The value of AQP4 expression within the border region was lower at 72 h (165 ± 24%, Fig. 4*F*) than the value at 24 h (220 ± 16%, Fig. 2*F*). Comparison of cortical and striatal regions showed decreased AQP4-IR in the ipsilateral regions (Fig. 4*F*). These findings suggest that the AQP4 expression was beginning to normalize within the border zone when the ADC and T2 values were starting to increase within this region.

In the striatum, the decrease of AQP4-IR at low magnification was confirmed at the cellular level (data not shown). This absence of labeling in the striatum correlates with cell death at this time. In the ipsilateral cortex, AQP4-IR was observed in reactive astrocytes with staining in astrocyte end-feet and also on whole cell bodies (Fig. 5, *A1* and *A2*). In contrast, the increase of AQP4-IR was observed around blood vessels in the border regions (Fig. 5*B*) but not in the contralateral cortex (Fig. 5, *C* and *D*). The gradient in AQP4 induction observed at 24 h was not maintained at 72 h (Fig. 5, *C* and *D*).

28 days. While many studies have examined the early events related to ischemic injury, we assessed whether the early MRI/immunohistochemistry changes were maintained or altered after the formation of a permanent region of injury. The DWI and ADC changes were reduced and appeared to normalize within the cortex (Fig. 6, *A* and *D*). However, there was reduced DWI signal intensity and increased ADC in the striatum (82%) and border region (30%) compared with the contralateral cortex ($p < 0.001$). These increases in ADC in ischemic tissue have been reported previously for acute lesions, however, ADC values were increased in the striatum

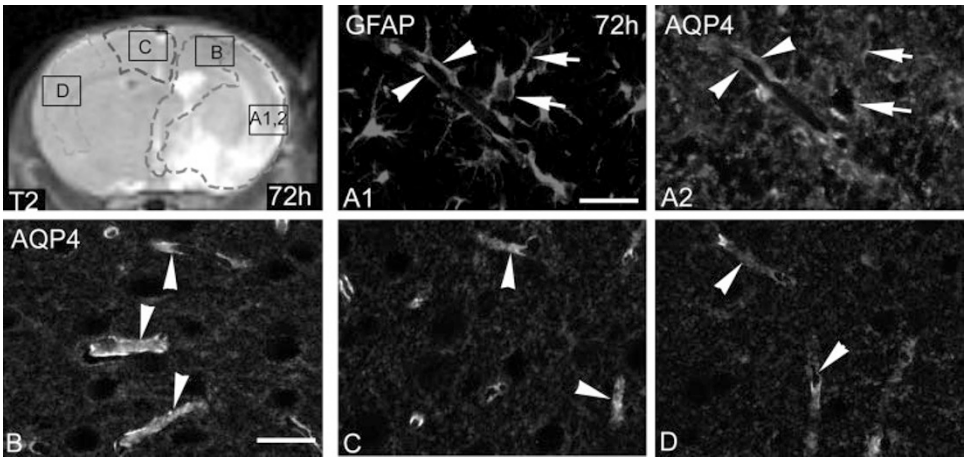

Figure 5. (*A*) A T2WI at 72 h with the same regions used for analysis at 24 h. (*B*) GFAP-staining (*A1*) was co-localized with AQP4-IR (*A2*) around blood vessels (*arrowheads, A1, A2*) and on astrocytic processes (*arrows, A1, A2*) in the ipsilateral cortex. (*B*) In the ipsilateral frontal cortex, the intensity of AQP4-IR was significantly increased only around blood vessels (*arrowheads*). (*C, D*). In the frontal (*C*) and the parietal (*D*) cortex of the contralateral hemisphere the intensity of AQP4-IR (*arrowheads, C, D*) was lower than to the ipsilateral regions (*arrowheads, B, D*). Bar: *A–D* = 40 μm.

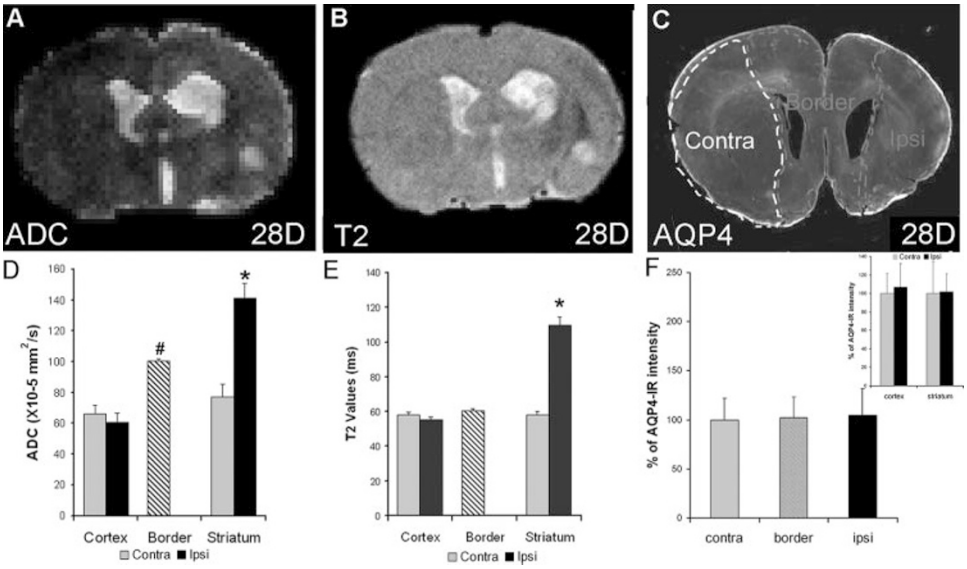

Figure 6. Comparison of MRI and AQP4-IR at 28 d after ischemia. (*A*) The ADC-image showed only slightly decreased signal intensity within the striatum and increased intensity in the cortex. (*B*) The T2WI at 28 d after ischemia showed increased ventricle size ipsilateral to the lesion. In addition, there was decreased signal intensity in the striatum of these animals. (*C*) Illustration of the AQP4-IR intensity with no observable changes. (*D*) The ADC values were now elevated within the striatum but unchanged in the cortex, indicating increased water content. (*E*) Similarly, T2 values were significantly elevated in the striatum but not the cortex. (*F*) Quantification of AQP4 expression revealed no change in cortex or striatum.

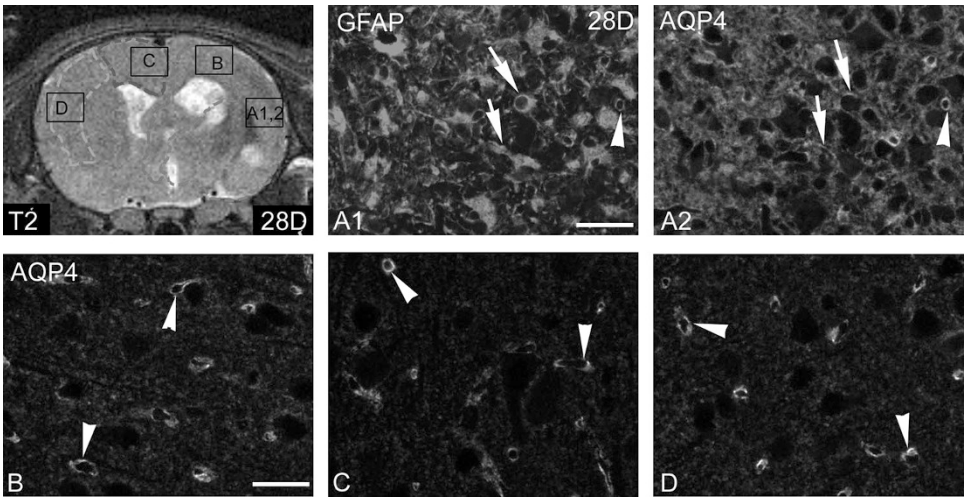

Figure 7. (*A*) A T2WI at 28d with the same regions used for analysis at 24 h. Intense GFAP-staining (*A1*) co-localized with AQP4-IR (*A2*) around blood vessels (*arrowheads*) and on processes (*arrows*) within the glial scar localized in the ipsilateral cortex. GFAP-IR (*A1*) and AQP4-IR (*A2*) was still elevated compared with the nonischemic tissues, the ipsilateral (*B*) and contralateral frontal cortex (*C*) and contralateral parietal cortex where AQP4-IR was observed around blood vessels in (*arrowheads*). Bar: *A–D* = 40 μm.

suggestive of ongoing tissue modifications (15). The cortical T2WI values also normalized at 28 d, suggesting that cortical alterations were minimal (Fig. 6, *B* and *E*). In contrast, striatal T2 values remained increased by 90% compared with the contralateral striatum ($p < 0.001$). The observations in the striatum are similar to those observed at 72 h. Thus, the neuroimaging data suggest that the striatal damage seen at 72 h is relatively permanent.

AQP4-IR at 28 d ($n = 3$) revealed that the changes seen at the earlier time points returned to normal, as evidenced by no significant changes in any of the regions evaluated (Fig. 6, *C* and *F*). However, at the cellular level, AQP4 labeling (Fig. 7, *A2*) was

still present in GFAP-positive reactive astrocytes (Fig. 7, *A1*) within the ipsilateral cortex and striatum (Fig. 7, *A1* and *A2*). Similarly, at 72 h, AQP4 labeling was observed on whole astrocyte cell bodies and on astrocyte end-feet revealed by an intense GFAP labeling, in contrast with the AQP4-IR observed in noninjured tissues (Fig. 7, *B-D*). Induction of AQP4-IR around blood vessels was not seen at 28 d (Fig. 7, *B–D*) despite a 30% increase in ADC within the border ($p < 0.001$).

DISCUSSION

Brain edema is a serious complication of stroke and significantly affects long-term morbidity (16). Brain AQP provide specific water routes through the plasma membrane. Although the consequences of increased AQP expression are not clearly understood, it is believed that AQP have an important role in the formation of cytotoxic edema and in the resolution of vasogenic edema (9). After focal ischemia in adult mice, induction of astrocytic AQP4 expression correlates with the temporal evolution of edema, suggesting an important role for AQP4 (9). A unique finding in the current study was the absence of edema formation (ADC and T2WI) in brain regions with the greatest levels of AQP4 expression. These findings suggest that, in the 10-d-old rat pup undergoing tfMCAO, tissue preservation may be related to the enhanced ability to increase water clearance in border regions.

As visualized by MRI, cytotoxic edema usually precedes the development of vasogenic edema (6,17,18). Deletion of AQP4 appears protective against the development of cytotoxic edema and results in smaller infarct volumes (10). Because cytotoxic edema occurs early (*i.e.* <24 h), it is unlikely that treatments designed to reduce AQP4 levels early after ischemia would be practical, particularly in newborns in whom the diagnosis of stroke is frequently delayed. In the current study, decreased ADC and increased T2WI values were found in the cortex and striatum at 24 h and likely reflect the development of cytotoxic as well as vasogenic edema. Indeed, the 24 h period may be a transitional period from cytotoxic to vasogenic edema as evidenced by our MRI and AQP4-IR results. In the regions bordering the ischemic cortex and striatum, AQP4 expression was substantially increased at 24 h and AQP4 induction was observed on astrocyte end-feet in contact with intraparenchymal vessels as previously described in tfMCAO in adult mice (9). Modifications of AQP4 expression in cerebral ischemia show decreased AQP4 expression in ischemic regions at 24 h after 90 min MCAO occlusion (19) and in the HII in 1- and 4-wk-old rat pups (7). Meng and colleagues (7) showed that AQP4 expression correlated with increased T2 and decreased ADC values reflecting edema formation at 24 h. Our results have similar MRI changes (*i.e.* decreased ADC, increased T2) but we observed increased AQP4-IR in the border region. The relative differences between the two models may be due to the fact that in the tfMCAO model the contralateral hemisphere does not appear to be affected in contrast to the HII, in which global cerebral hypoxia is used (18). Furthermore, the ischemic lesion size is also greater in the HII model than in the focal tfMCAO model (13,18).

At 72 h, we found decreased AQP4 expression in the ipsilateral striatum and cortex (Fig. 3), similar to that seen at 24 h in previous studies (7). T2WI and ADC values were returning to baseline in ipsilateral regions. As in previous studies, the MRI decrements do not necessarily translate to cessation of ongoing neuropathology, in particular DWI (20). AQP4 expression was also returning toward baseline by 72 h and reached normal values by 28 d. The highest variations in T2 and ADC values were not seen in the border regions where AQP4 expression was significantly increased at 24 h. This important observation suggests that AQP4 induction on astrocyte end-feet does not promote edema formation in these border regions. This observation also suggests that AQP4 induction does not facilitate increases in tissue water content but may influence removal of excess water from at-risk tissue. Recently, it has been suggested (11) that induction of AQP4 on astrocyte end-feet may facilitate diffusion of water toward the vascular compartment. AQP4 deletion promotes the development of vasogenic edema by decreasing water clearance (11). These data agree with a recent pharmacological study in a model of traumatic brain injury showing that sulphoraphane-induced expression of AQP4 correlated with decreased brain water content (12). Together, these observations suggest that up-regulation of AQP4 expression with pharmacological tools might be beneficial in reducing vasogenic edema and mitigating its unwanted effects.

Increased AQP4 expression was observed at 28 d in reactive astrocytes involved in astrogliosis. Intense AQP4 labeling in reactive astrocytes at 72 h suggests that gliosis is initiated at 72 h after stroke. In reactive astrocytes, AQP4 expression was observed on the entire cell, in accordance with previous results in adult mice (9,21). Induction of AQP4 in reactive astrocytes may facilitate migration of cells during glial scar formation (21). This increased AQP4 expression in reactive astrocytes was still present at 28 d and could facilitate adhesion between cells. It was recently shown that increased expression of AQP4 facilitated adhesion between reactive astrocytes and promoted water movements within the glial scar (22).

In conclusion, our observations suggest that induction of AQP4 in border regions may limit edema formation that occurs later after injury (*i.e.* 24–72 h) and preserve tissue. Agents that stimulate AQP4 expression may assist in water clearance from brain parenchyma and could improve neurologic outcomes of neonates with HII or stroke. This may be of particular interest in newborns, as the brain water content of the neonatal brain is substantially greater than later in life (23).

Acknowledgments. The authors thank Mr. S. Chong for assistance with the neuroimaging and Mrs. M. F. Hamou for assistance with immunohistochemistry.

REFERENCES

1. Lynch JK, Hirtz DG, DeVeber G, Nelson KB 2002 Report of the National Institute of Neurological Disorders and Stroke workshop on perinatal and childhood stroke. Pediatrics 109:116–123
2. De Vries LS, Van der Grond J, Van Haastert IC, Groenendaal F 2005 Prediction of outcome in new-born infants with arterial ischaemic stroke using diffusion-weighted magnetic resonance imaging. Neuropediatrics 36:12–20

3. Kuker W, Mohrle S, Mader I, Schoning M, Nagele T 2004 MRI for the management of neonatal cerebral infarctions: importance of timing. Childs Nerv Syst 20:742–748
4. Krishnamoorthy KS, Soman TB, Takeoka M, Schaefer PW 2000 Diffusion-weighted imaging in neonatal cerebral infarction: clinical utility and follow-up. J Child Neurol 15:592–602
5. Rumpel H, Ferrini B, Martin E 1998 Lasting cytotoxic edema as an indicator of irreversible brain damage: a case of neonatal stroke. AJNR Am J Neuroradiol 19:1636–1638
6. Loubinoux I, Volk A, Borredon J, Guirimand S, Tiffon B, Seylaz J, Meric P, Rosenberg GA 1997 Spreading of vasogenic edema and cytotoxic edema assessed by quantitative diffusion and T2 magnetic resonance imaging. Stroke 28:419–427
7. Meng S, Qiao M, Lin L, Del Bigio MR, Tomanek B, Tuor UI 2004 Correspondence of AQP4 expression and hypoxic-ischaemic brain oedema monitored by magnetic resonance imaging in the immature and juvenile rat. Eur J Neurosci 19:2261–2269
8. Badaut J, Hirt L, Granziera C, Bogousslavsky J, Magistretti PJ, Regli L 2001 Astrocyte-specific expression of aquaporin-9 in mouse brain is increased after transient focal cerebral ischemia. J Cereb Blood Flow Metab 21:477–482
9. Ribeiro Mde C, Hirt L, Bogousslavsky J, Regli L, Badaut J 2006 Time course of aquaporin expression after transient focal cerebral ischemia in mice. J Neurosci Res 83:1231–1240
10. Manley GT, Fujimura M, Ma T, Noshita N, Filiz F, Bollen AW, Chan P, Verkman AS 2000 Aquaporin-4 deletion in mice reduces brain edema after acute water intoxication and ischemic stroke. Nat Med 6:159–163
11. Papadopoulos MC, Manley GT, Krishna S, Verkman AS 2004 Aquaporin-4 facilitates reabsorption of excess fluid in vasogenic brain edema. FASEB J 18:1291–1293
12. Zhao J, Moore AN, Clifton GL, Dash PK 2005 Sulforaphane enhances aquaporin-4 expression and decreases cerebral edema following traumatic brain injury. J Neurosci Res 82:499–506
13. Ashwal S, Tone B, Tian HR, Chong S, Obenaus A 2006 Serial magnetic resonance imaging in a rat pup filament stroke model. Exp Neurol 202:294–301
14. Wong SK 2004 A 384-well cell-based phospho-ERK assay for dopamine D2 and D3 receptors. Anal Biochem 333:265–272
15. Schaefer PW, Hunter GJ, He J, Hamberg LM, Sorensen AG, Schwamm LH, Koroshetz WJ, Gonzalez RG 2002 Predicting cerebral ischemic infarct volume with diffusion and perfusion MR imaging. AJNR Am J Neuroradiol 23:1785–1794
16. Klatzo I 1985 Brain oedema following brain ischaemia and the influence of therapy. Br J Anaesth 57:18–22
17. Gartshore G, Patterson J, Macrae IM 1997 Influence of ischemia and reperfusion on the course of brain tissue swelling and blood-brain barrier permeability in a rodent model of transient focal cerebral ischemia. Exp Neurol 147:353–360
18. Ashwal S, Tone B, Tian HR, Chong S Obenaus A 2007 Comparison of two neonatal ischemic injury models using magnetic resonance imaging. Pediatr Res 61:9–14
19. Amiry-Moghaddam M, Otsuka T, Hurn PD, Traystman RJ, Haug FM, Froehner SC, Adams ME, Neely JD, Agre P, Ottersen OP, Bhardwaj A 2003 An alpha-syntrophin-dependent pool of AQP4 in astroglial end-feet confers bidirectional water flow between blood and brain. Proc Natl Acad Sci U S A 100:2106–2111
20. Ringer TM, Neumann-Haefelin T, Sobel RA, Moseley ME, Yenari MA 2001 Reversal of early diffusion-weighted magnetic resonance imaging abnormalities does not necessarily reflect tissue salvage in experimental cerebral ischemia. Stroke 32:2362–2369
21. Saadoun S, Papadopoulos MC, Watanabe H, Yan D, Manley GT, Verkman AS 2005 Involvement of aquaporin-4 in astroglial cell migration and glial scar formation. J Cell Sci 118:5691–5698
22. Hiroaki Y, Tani K, Kamegawa A, Gyobu N, Nishikawa K, Suzuki H, Walz T, Sasaki S, Mitsuoka K, Kimura K 2006 Implications of the aquaporin-4 structure on array formation and cell adhesion. J Mol Biol 355:628–639
23. Sulyok E 2006 Physical water compartments: a revised concept of perinatal body water physiology. Physiol Res 55:133–138